



Predictive modeling of drilling machine performance for jute fiber-reinforced polymer composites using GA, TLBO, and GRA-based RSM approaches

Lokesh Kumar¹ · Ashish Goyal¹ · Sudesh Garg² · Rakesh Kumar Phanden³

Received: 6 February 2024 / Accepted: 9 May 2024

© The Author(s), under exclusive licence to Springer-Verlag France SAS, part of Springer Nature 2024

Abstract

Machining the surface of polymer composites is an inevitable task for components. Hole-making processes like milling or drilling can be conducted to analyze a range of parameters concerning the polymer composite. Specific techniques have revealed that machinability in polymers is challenging due to their high hardness. This research investigated thrust as well as surface roughness measurements on jute fiber-reinforced polymer composites utilising different drill bit diameters, studying parameter interactions via 3-D surface plots. In contrast, optimal process parameters were predicted using the Response Surface Methodology (RSM), Grey Relational Analysis (GRA), Genetic Algorithm (GA), and Teaching learning-based optimization (TLBO) curve. GRA-based RSM was instrumental in crafting optimal fitness regression models for the GA and TLBO of polymer composites reinforced with jute fibers. Both, the RSM and TLBO methods exhibited significant correspondence over experimental results. According to these outcomes, thrust force was often shown to enhance with low spindle speed, high feed rate, and small drill diameter. When spindle speed, feed, and tool diameter are reduced, surface roughness decreases. This study holds practical significance by offering a clear pathway to minimize thrust force and surface roughness during drilling operations, consequently enhancing process quality and efficiency.

Keywords Polymer composite · Response surface methodology · GRA · Optimization · Drilling machine performance

1 Introduction

Fiber-reinforced polymers (FRPs) represent a prominent category of composites widely employed for structural applications owing to their favorable ratio of strength-to-weight [31]. Recent advancements have seen the replacement of traditional biomaterials with synthetic fibers, aiming to bolster mechanical properties. Drilling is essential to the manufacturing process, a procedure pivotal for creating apertures in

structural components. Notably, research by Kumar et al. [21] highlights the significant persuade of spindle feed rate on thrust force as well as the drill diameter during drilling operations. Moreover, feed rate and spindle speed exert considerable impact on surface roughness. A comprehensive understanding of drilling dynamics within natural fiber-reinforced polymers was pursued by Vinayagamoorthi et al. [41], who examined various parameters in particular tool diameter, feed rate, point angle, and speed too. The study elucidated crucial output parameters during drilling operations, including thrust force, torque, and deflection. A study was conducted to establish an empirical model, employing a central composite design, thereby contributing to the understanding and optimising of drilling processes in FRPs.

Heidary et al. [13] analyzed thrust action, delamination, and residual flexural stability in drilling knit E-glass fiber-epoxy matrices reinforced with functionalized multi-walled carbon nanotubes. Consequently, the feed rate was the most influential factor in thrust action and delamination, followed by spindle speed. Paneerselvam et al. [29] demonstrated a study on the effect of delamination during drilling on

✉ Ashish Goyal
ashish.goyal@jaipur.manipal.edu

Rakesh Kumar Phanden
rkp.doctor@gmail.com; rkphanden@amity.edu

¹ Department of Mechanical Engineering, Manipal University Jaipur, Jaipur, Rajasthan 303007, India

² Department of Mechanical Engineering, Swami Keshvanand Institute of Technology, Management, and Gramothan, Jaipur, India

³ Department of Mechanical Engineering, Amity University Uttar Pradesh, Noida, India

Sisal-Glass Fibres Reinforced Polymeric (S-GFRP) matter. Taguchi's approach was followed to investigate delamination. *S/N* ratios were utilized to refine the operating parameters for minimizing delamination. Two distinct approaches, specifically profile projector and computational imaging, determined the delamination, which yielded reliable results.

Antil et al. [1] discovered that grey rational analysis (GRA) emerged as a convincing optimization technique, significantly improving the manufacturing sector. They utilized SiC-reinforced polymer to optimize process parameters using the micro drilling process, resulting in enhanced quality, in particular, improved material removal rate (MRR) with minimal cutting and taper. Soepangkat et al. [38] explored a method aiming for diverse performance attributes, including optimum torque (*Mz*), thrust force (*Fz*), delamination (*D*), hole roundness (*R*) as well as hole surface roughness (*Ra*), during the drilling of fiber-reinforced polymers. Through a series of trials, they found that the BPNN-based GA maximal evaluation strategy notably enhanced and predicted multiple performance aspects, as confirmed by subsequent trials.

Maleki et al. [34] examined various attributes of woven jute fiber-reinforced polymer through drilling process. Various cutting parameters were examined and evaluated, including drill bit types, thrust force, surface roughness, etc. A statistical evaluation approach was used to determine the proportional contributions of these factors. Finally, results indicated that drill bit type affected other characteristics. Kaviarasan et al. [17] aimed to investigate the dry-condition characteristics of Delrin polymer to achieve a high surface finish. They applied the L27 orthogonal array to drilling conditions, wear mechanisms, types of wear, and wear measurement techniques. As a result, this study has impacted the comprehension of the long-term implications of composite material machining wear and the identification of protective measures against accelerated drill wear.

Ismail et al. [14] conducted a thorough investigation into tool wear in fiber-reinforced polymeric composites. Their study covered types and mechanisms of tool wear, drilling environments, measurement methods, preventive measures against rapid drill wear as well as the impacts on composite material machining. The researchers also provided insights into future perspectives on tool wear. Shunmugesh et al. [37] employed Taguchi Grey Research Analysis for various drill bits and conducted trials in order to increase machining conditions and reduce delamination factor. Results were concluded by comparing percentage parts of selected factors.

Ramesh et al. [32] employed thin laminated composites, widely utilized in small-scale engineering tasks, and contrasted them with thick laminated composites. Their findings revealed that the blended drill bit surpassed standard drill bit in performance. Feito et al. [10] investigated cutting tool flaws in CFRP polymer through a three-step approach. The initial phase involved conducting a complete factorial DOE

to assess importance of individual parameter of process and the relations with additional criteria, notably delamination at both positions, that is, hole entry and exit, as well as at thrust force and torque. In subsequent phases, they employed ANOVA and RSM, respectively, aimed to derive conclusions with minimal possible cutting tool damage. Jayabal et al. [15] studied the effect of cutting tool parameters such as the diameter of the drill bit, feed rate, and spindle speed. They employed Box–Behnken design, Nelder–Mead, and GA techniques in the study, aiming to enhance the cutting phase of the tool and reduce tool wear.

Mercy et al. [25] investigated a material's capacity for self-healing in the event of damage discovery. Glass fiber-reinforced epoxy resin was mixed with microcapsules containing dicyclopentadiene-monomer to create self-healing GFRP samples. Drilling was performed while thrust force and temperature readings were being taken simultaneously, and it was determined that the microcapsule concentration had produced the required results for both observed parameters. In many practices involving PA6 and PA6-NC nanocomposites, Yazdi et al. [39] employed the thrust force modeling approach to determine thrust force values using a two mm-diameter high-speed steel drill with a 118-degree point angle. The PSNN algorithm was also used to create a thrust force prediction model, utilizing a particle-swarm-optimization-based neural network (PSNN) with fine-high setup parameters for drilling PA6 nano clay (NC) nanocomposite material. The outcome ultimately concluded that the amount of NC content in PAC composite would significantly decrease the thrust force.

Uysal et al. [40] investigated tool wear conditions in a sheet molding composite (SMC) consisting of 45 weight percent calcium carbonates, 25 weight percent polyester, and 30 weight percent glass fiber in a study published in 2012. Several feed combinations, drill point angles, and cutting speeds were chosen during the drilling operation. Taguchi DOE and ANOVA were employed to find a best combination of cutting parameters, including the investigation of consequences of tool wear. Chip volume served as an additional criterion for comparing the collected data. The results evidenced that increasing feed and lowering the drill tip angle lessened tool wear Babu et al. [3]. conducted drilling trials on blended glass-carbon fiber-reinforced (GCFR) epoxy composites via a manual layup process to evaluate manufacturing attributes, including torque, thrust force, delamination, and surface roughness. They investigated the impact of spindle speed, drill diameter, and feed rate as drilling process variables. The statistical analysis unveiled drill diameter as the primary parameter of significance, trailed by feed rate and spindle speed.

Pultruded glass fiber-reinforced polymer composite (PGFRP) with hybrid filler, produced at optimal pultrusion settings, was constructed by Gupta et al. [12]. The effects

of drilling parameters, including feed rate, spindle speed, and drill bit lip angle, on the delamination aspect of PGFRP composites with hybrid filler have been examined. Taguchi's single-response optimization technique was utilized to determine the optimal drilling parameters. Upon synthesizing PGFRP of a specific composition, it was discovered that achieving the highest delamination aspect required a spindle speed of 3000 rpm, a feed rate of 200 mm/min, and a twist drill with a lip angle of 1000.

Saravankumar et al. [35] investigated the thrust force and surface roughness of composites reinforced with snake grass fibers. Drilling diagnostic procedures were executed to assess the factor effect on the thrust force of drilled unidirectional snake grass fiber-reinforced synthetic materials. It was found that a spindle speed of 1800 rpm, a feed rate of 10 mm/min, and a drill diameter of 4 mm developed the maximal thrust force value. Ramesh et al. [33] explored how different drill bit coating materials, along with controlled variables such as drill bit speed and feed rate, affected surface quality in epoxy composites reinforced with glass fiber and nano granite powder. The trials utilized the Taguchi L9 rotationally symmetric array, and the statistical analysis employed ANOVA to align the process's response parameters with the radial drilling criteria. The tests' findings demonstrated that the two significant aspects impacting the effectiveness of the drilled hole are high spindle speeds and a drill bit coated in bronze oxide. Niranjana et al. [26] examined how different drill types (slot, twist, and braid) and process variables (feed rate and machining speed) affected hole quality errors in GFRP composite drilling. They assessed roundness error, machined area roughness, delamination, and diameter deviation. Using TOPSIS, they prioritized parameters to minimize errors, finding that a spur-type drill with a broader spindle speed range yielded superior hole quality.

Fedai et al. [9] employed the GRA technique to improve various aspects of drilling in GFRP composites, including the weight percentage of multi-wall carbon nanotubes (MWCNTs), cutting speed, and feed rate, with a focus on thrust force and delamination. Through statistical ANOVA, they observed the impact of drilling parameters on multiple responses. Subsequently, the optimal parameters were identified as 1% MWCNTs, a cutting speed of 25 m/min, and a feed rate of 0.10 mm/rev, aimed at minimizing both thrust force and delamination simultaneously. Consequently, they emphasized the significance of the feed rate in the drilling process.

Antil et al. [2] applied multi-objective particle swarm optimization (MOPSO) to optimize parameters for electrochemical discharge drilling in SiCp and glass fiber-reinforced polymer matrix composites (PMCs). The planned procedure was centered on the central composite concept and utilized RSM. Factors considered were electrolyte concentration, interelectrode gap, duty factor, and voltage, while

objective quality characteristics (OQCs) comprised material removal rate (MRR) and overcut. The empirical findings underwent refinement through an RSM-based desirability structure and were further optimized with MOPSO to attain the most favorable MRR and minimal overcut. Comparative analysis illustrated MOPSO's efficacy in enhancing OQCs.

Babu et al. [3] utilized a Taguchi L9 orthogonal array to execute drilling endeavours in the design of scientific studies. A fuzzy logic optimization tool was implemented to determine performance characteristics such as thrust force, torque, and delamination factor in the drilling of CFRP composite. There were signs of excellent accordance between the fuzzy results and the experimental norms. As a result, an ANOVA assessment was conducted to identify significant criteria during the drilling of CFRP hybrid material. Erturk et al. [7] investigated drillability using a range of drill bits, feed rates, and spindle speeds. They modified the tool-composite interface for dry drilling experiments and employed image analysis to assess delamination. The study found that tool coating influenced drilling mechanics, with conclusions validated using response surface methodology. Optimal parameters identified were a feed rate of 0.13 mm/rev, spindle speed of 2425 rpm, and HSS-TiN drill bit.

Jayaprakash et al. [16] investigated the impact of including rice husk in epoxy-based composite plates on drilling specifications. The findings demonstrated that inserting rice husk substantially enhances the composites' strength. In addition to strengthening the matrix, rice husk functions as a lubricant, facilitating machining. This investigation revealed that organic fillers may be deployed to improve drilled hole quality at a lower expense. Palanikumar et al. [27] provided a helpful strategy to maximize drilling configurations with different performance criteria. It used Gray relational analysis and was based on Taguchi's strategy. Taguchi's L16, 4-level orthogonal array was adopted in scientific research. While optimizing the drilling parameters, consideration is given to the delamination aspect, workpiece surface roughness, thrust action, and other performance characteristics, including feed rate and spindle speed. Thus, Gray relational grade analysis shows that the feed rate has a much more significant impact than the spindle speed. These results establish that this approach can potentially increase the efficacy of drilling activities.

Babu et al. [3] focused on the hand layup technique of drilling hybrid glass-carbon fiber-reinforced (GCFR) epoxy composites. An artificial intelligence or fuzzy inference system was used to mitigate the precision effect caused by individual optimal characteristics. Geier et al. [11] conducted optimization of machining parameters through an evaluation of the machinability of hand-laminated uni-directional CFRP. This evaluation involved the utilization of a solid

carbide end mill for helical milling and a distinctive diamond-coated twist drill. They conducted experimental investigations on thin CFRP laminates using a K20 carbide drill, as described by Krishnaraj et al. [19], altering drilling settings based on a full factorial design. Peel-up, push-out, circularity, and hole diameter were key metrics for hole quality examined. ANOVA determined contribution rates of these metrics. The genetic algorithm (GA) approach facilitated objective modifications to identify optimal cutting conditions for flawless drilling.

Kharwar et al. [18] highlighted the crucial role of process constraints and developing a potent optimization plan while drilling multiwall carbon nanotubes and epoxy nanocomposites. Based on completed pilot tests and available literature, the variables considered were MWCNT%, drill bit speed, feed rate, and drill bit materials (HSS, carbide, and TiAlN). Several researchers have encountered difficulties while trying to manufacture polymer composites. It is challenging to achieve boosted surface polish and other characteristics. The present work aims to enhance the thrust force and surface roughness during machining a polymer composite reinforced with jute fiber. The drilling operation is carried out using the BPNN model, which has been optimized by applying response surface techniques and grey relational analysis to determine the impact of process factors on responses. The evaluation of substantial and insignificant criteria was also done using the ANOVA strategy.

This study aims to enhance and analyze the drilling performance of jute fiber-reinforced composites. Input variables including drill bit diameter, spindle speed, and feed rate were chosen, while drilling properties are evaluated based on output responses such as thrust force and surface roughness. ANOVA and RSM are utilized to analyze the drilling variables, and experimental data are employed to determine optimal parameter settings using machine learning. Finally, a comparison is made between the experimental data obtained from BBD and machine learning techniques.

Section 2 delves into the materials and methodology, outlining the experimental plan (2.1) and utilising GRA (2.2) to analyze the correlation between various parameters and drilling performance. In Sect. 3, results and discussion, the analysis of thrust force (3.1) and surface roughness (3.3) is presented, supplemented by ANOVA analysis for both thrust force (3.2) and surface roughness (3.4). Regression equations for thrust force and surface roughness are also established (3.5). Furthermore, the section covers GA optimization (3.6) and TLBO algorithm (3.7) applications to enhance drilling performance. A comparative investigation of the projected outcomes of GRA with GA and TLBO predicted outcomes is also discussed (3.8). Finally, in Sect. 4, the conclusion and recommendations are presented.

2 Materials and methodology

The current experimental study conducted drilling operations on jute fiber-reinforced polymer composites. Three twist drill cutting tools made of HSS, with diameters of 6 mm, 7 mm, and 8 mm, were selected, along with varying spindle speed combinations. The drilling operation took place at the machine shop of Manipal University Jaipur, India, utilizing a radial drilling machine. Input parameters included drill bit diameter, spindle speed, and feed rate. A rectangular workpiece measuring 11.5 cm × 7.5 cm × 8 mm was employed for hole fabrication in the jute fiber composites. The chemical composition of the specimen comprises cellulose (64.4%), hemicellulose (12%), lignin (11.8%), pectin (0.4%), wax (0.5%), and moisture content (1.1%).

In the present work, dry machining was employed during hole fabrication, so no coolant is required because if any coolant were used, the jute fibre would absorb it. Some particles would adhere to the drill bit, creating uneven hole surfaces. In this study, thrust force and surface roughness were evaluated as response variables. Surface roughness was quantified utilizing Mitutoyo's SurfTest (SJ-210), while thrust force was measured employing Unitech Scales Measuring Equipment (Model 6340). The hardness of the specimen is observed as 74 HRA at the Rockwell scale.

The process parameters have been selected based on trial practices and review work, Palanikumar et al. [28]. Table 1 displays the various stages of process specifications.

2.1 Plan of experiments

Stiff clamping attachments were utilized to affix the dynamometer firmly to the worktable of the machining center, ensuring stability against vibrations. Subsequently, the polymer composite material was securely strapped onto the dynamometer. The experiments were conducted under natural cutting conditions (Tables 2 and 3). Throughout the study, drilling thrust force was monitored using a dynamometer and a synchronized charge amplifier. The collected signals were then transmitted to data storage and acquisition software via a well-insulated link employing an A/D card converter. Prior to commencing any scientific investigations, all equipment

Table 1 Process specifications and their levels

| Input parameters | Levels | | |
|----------------------|--------|------|------|
| | L1 | L2 | L3 |
| Drill bit dia., (mm) | 6 | 7 | 8 |
| Spindle speed (rpm) | 600 | 1000 | 1400 |
| Feed rate, (mm/rev) | 30 | 60 | 90 |

Table 2 The L27 orthogonal array and their responses

| S. no | Drill (mm) | Spindle Speed | Feed rate (mm/min) | Thrust (Kgf) | Surface roughness (μm) |
|-------|------------|---------------|--------------------|--------------|-------------------------------------|
| 1 | 6 | 600 | 30 | 8.37 | 10.258 |
| 2 | 6 | 600 | 60 | 9.02 | 12.95 |
| 3 | 6 | 600 | 90 | 8.66 | 8.48 |
| 4 | 6 | 1000 | 30 | 13.75 | 11.01 |
| 5 | 6 | 1000 | 60 | 11.48 | 13.125 |
| 6 | 6 | 1000 | 90 | 14.08 | 9.09 |
| 7 | 6 | 1400 | 30 | 10.32 | 9.123 |
| 8 | 6 | 1400 | 60 | 9.73 | 12.459 |
| 9 | 6 | 1400 | 90 | 9.56 | 11.375 |
| 10 | 7 | 600 | 30 | 18.96 | 13.623 |
| 11 | 7 | 600 | 60 | 19.43 | 9.22 |
| 12 | 7 | 600 | 90 | 20.28 | 8.694 |
| 13 | 7 | 1000 | 30 | 21.68 | 13.025 |
| 14 | 7 | 1000 | 60 | 21.12 | 12.937 |
| 15 | 7 | 1000 | 90 | 20.98 | 14.038 |
| 16 | 7 | 1400 | 30 | 19.93 | 17.072 |
| 17 | 7 | 1400 | 60 | 18.72 | 8.048 |
| 18 | 7 | 1400 | 90 | 20.41 | 10.203 |
| 19 | 8 | 600 | 30 | 7.69 | 10.023 |
| 20 | 8 | 600 | 60 | 8.07 | 9.983 |
| 21 | 8 | 600 | 90 | 9.13 | 11.863 |
| 22 | 8 | 1000 | 30 | 10.31 | 12.98 |
| 23 | 8 | 1000 | 60 | 9.83 | 11.479 |
| 24 | 8 | 1000 | 90 | 12.08 | 12.284 |
| 25 | 8 | 1400 | 30 | 6.92 | 9.623 |
| 26 | 8 | 1400 | 60 | 8.01 | 10.287 |
| 27 | 8 | 1400 | 90 | 7.33 | 11.294 |

underwent rigorous calibration. The experimental setup is illustrated in Fig. 1, while Fig. 2 displays the fabricated specimen.

2.2 Grey relational analysis

GRA is a statistical tool invented by Dr. Deng Julong in 1982. It analysed the relationship between the variables and attributes. This have belonged to the multi-criteria decision-making (MCDM) technique to evaluate the multiple attributes with experimental variables. Here, original experimental data is transferred into a comparability series showing the close or appropriate data value [22]. After that, it was normalised by dividing the data in the original series by 0 and 1. It shows the three quality criteria for attributes: larger, better, smaller, better, and nominal, which give optimal outcomes. In the present work, the smaller, the better

has been counted to observe the thrust and surface roughness responses. Following steps of GRA have been considered:

Let m be the total number of listed projects and n be the total number of impact factors. Next, an eigenvalue matrix, a $m \times n$ value matrix, is configured. The grey relationship methodology is depicted in Fig. 3.

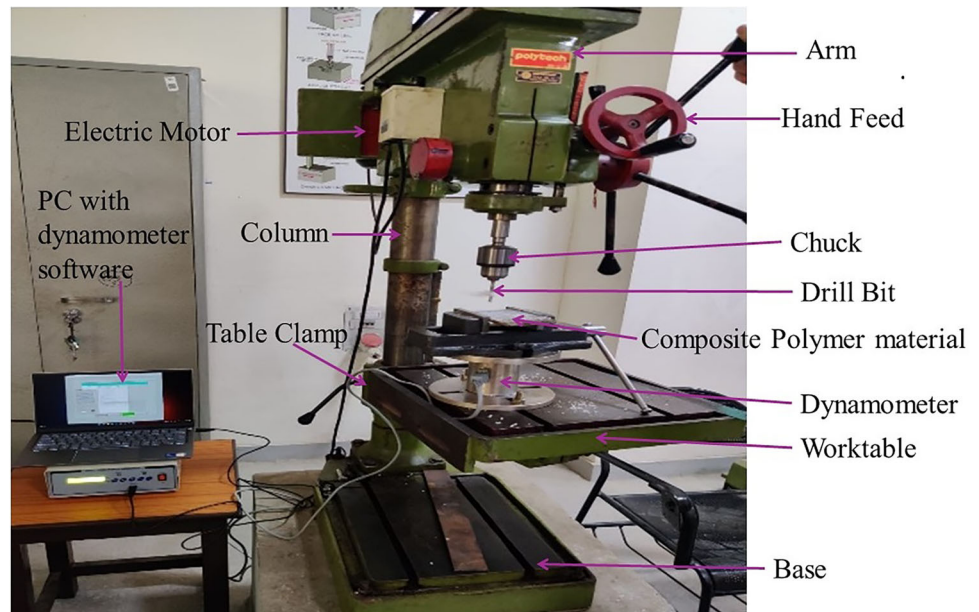
$$X = \begin{bmatrix} x_1(1), x_1(2), \dots, x_1(n) \\ x_2(1), x_2(2), \dots, x_2(n) \\ \dots \\ x_m(1), x_m(2), \dots, x_m(n) \end{bmatrix} \quad (1)$$

where $x_i(k)$ is the value of the number i listed project and the number k influence factors.

Table 3 Analysis of variance test for thrust force

| Source | Sum of squares | D.F | Mean square | F-value | P-value | |
|-----------------|----------------|-----|--------------------------|---------|----------|-------------|
| Model | 634.95 | 9 | 70.55 | 1204.56 | < 0.0001 | Significant |
| A-drill dia | 8.22 | 1 | 8.22 | 140.37 | < 0.0001 | Significant |
| B-Spindle speed | 0.3828 | 1 | 0.3828 | 6.54 | 0.0204 | |
| C-Feed rate | 1.9 | 1 | 1.9 | 32.46 | < 0.0001 | Significant |
| AB | 0.1482 | 1 | 0.1482 | 2.53 | 0.1301 | |
| AC | 0.5184 | 1 | 0.5184 | 8.85 | 0.0085 | |
| BC | 0.1764 | 1 | 0.1764 | 3.01 | 0.1007 | |
| A ² | 477.75 | 1 | 477.75 | 8157 | < 0.0001 | Significant |
| B ² | 31.51 | 1 | 31.51 | 537.94 | < 0.0001 | Significant |
| C ² | 8.42 | 1 | 8.42 | 143.79 | < 0.0001 | Significant |
| Residual | 0.9957 | 17 | 0.0586 | | | |
| Lack of fit | 0.9957 | 3 | 0.3319 | | | |
| Pure error | 0 | 14 | 0 | | | |
| Cor total | 635.95 | 26 | | | | |
| Std. dev | 0.242 | | R ² | 0.9984 | | |
| Mean | 17.83 | | Adjusted R ² | 0.9976 | | |
| C.V. % | 1.36 | | Predicted R ² | 0.9749 | | |
| | | | Adeq Precision | 91.3378 | | |

The Predicted R² of 0.9749 is in reasonable agreement with the adjusted R² of 0.9976; i.e. the difference is less than 0.2

Fig. 1 Experimental arrangement used in present work, using drill dynamometer

Step 1 Initially finding the S/N ratios from the original data values.

$$S/N(SB) = -10 \log_{10} \left[\left(\frac{1}{n} \sum X_{ij}^2 \right) \right] \quad (2)$$

where X_{ij} —is the output value that is considered. SB- is smaller the better criterion.

Step 2 Normalized values S/N ratios to find Z_{ik} for thrust and surface roughness.

$$Z_{ik} = \frac{\max x_i(k) - x_i(k)}{\max x_i(k) - \min x_i(k)} \quad (3)$$

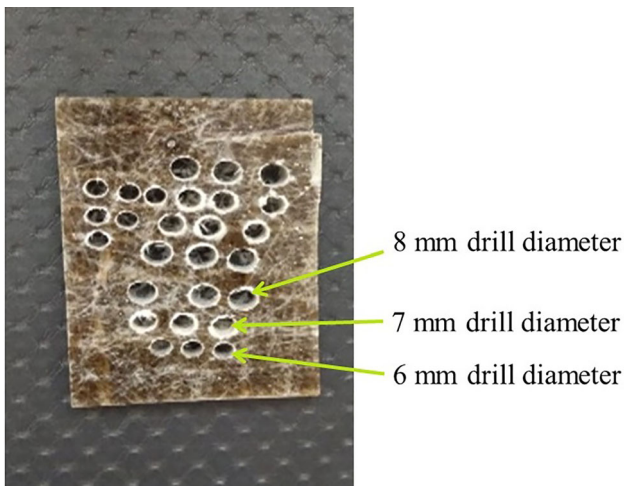


Fig. 2 Fabricated specimen

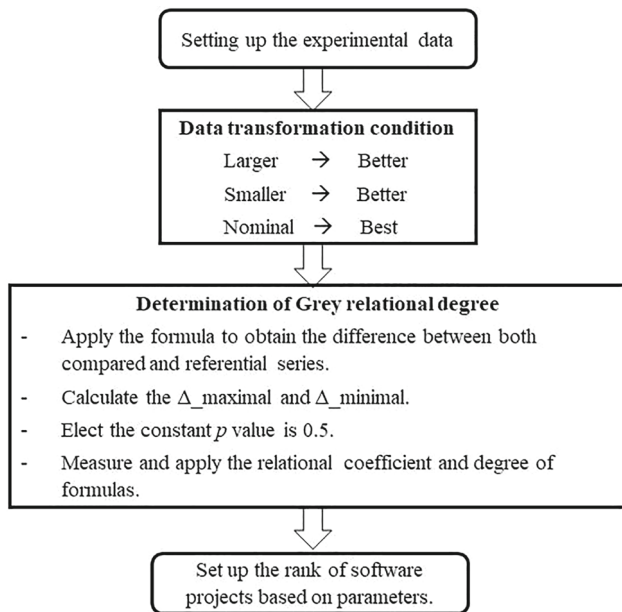


Fig. 3 The emergence of grey relation degree for software

Step 3 Deviation sequence find out Δx_{ij} and give $\Delta x_{Min} = 0, \Delta x_{Max} = 1$

$$\Delta x_i(k) = |x_0(k) - x_i(k)| \tag{4}$$

Step 4 Determine the Grey relational coefficient ξ for the normalized S/N ratios data and the distinguishing coefficient value p is 0.5.

$$\xi_i(k) = \frac{\Delta \min + p \Delta \max}{\Delta x_i(k) + p \Delta \max} \tag{5}$$

Step 5 Originate the grey relational grade r_i and rank. Here, $w(k)$ is the proportion of the number 'k' influence

factor to the total influence indicators.

$$r_i = \sum [w(k)\xi(k)] \tag{6}$$

Step 6 Analyse the optimal setting was chosen directly according to rank.

3 Result and discussion

3.1 Analysis of result for thrust force

Figure 4a depicts the spindle speed-drill interaction, revealing lower thrust force values with certain combinations. The minimum thrust, i.e., 10 Kgf, was obtained at a lower spindle speed and drill value, i.e., 800 rpm and 7 mm, respectively. The possible reason may be the lower feed rate at a drill value of 6 mm, 6.5 mm; hence, lower thrust force is attained. However, at the midpoint of the feed rate, a parabolic curve is shown due to a rise in higher spindle speed, which generates a high temperature during drill cutting on polymer composites. Beyond this, in Fig. 4b and c, higher thrust force has been produced gradually as the feed rate and spindle speed rise, indicating higher thermal energy losses at the interaction of drill diameter and composite material. Therefore, these various drill diameters in the initial drill stages (6 to 8 mm) have been influential in gradually increasing the spindle speed and feed rate, which depicted a lesser thrust force in Fig. 4. Due to this, chip evacuation with a lower cutting drill diameter showed regularity and smoothness in the drilling of composite polymer, which directly controlled the hole surface quality.

Figure 5 represents the cubic illustration of the thrust force with three levels of input variables. It tends to keep one input parameter varying while the other two input parameters remain constant at a cube plot of the response thrust force. This means that the thrust force variation lies between 9.61 and 10.10 Kgf, which provides an optimal setting at distinct levels of inputs. However, these representations show the increased or decreased median of thrust force on the cube plot of the machining variable.

Figure 6 shows the predicted vs. actual plot of thrust force (Kgf). The data lie straight, indicating that the model is acceptable. The normal probability plot for thrust force is also shown in Fig. 6. All of the residuals are presented as being on a straight line. This might be regarded as the current model's fitness. It also indicates no residual clustering and that all errors have a normal distribution. This suggests that every variable chosen for the current investigation contributes to the model.

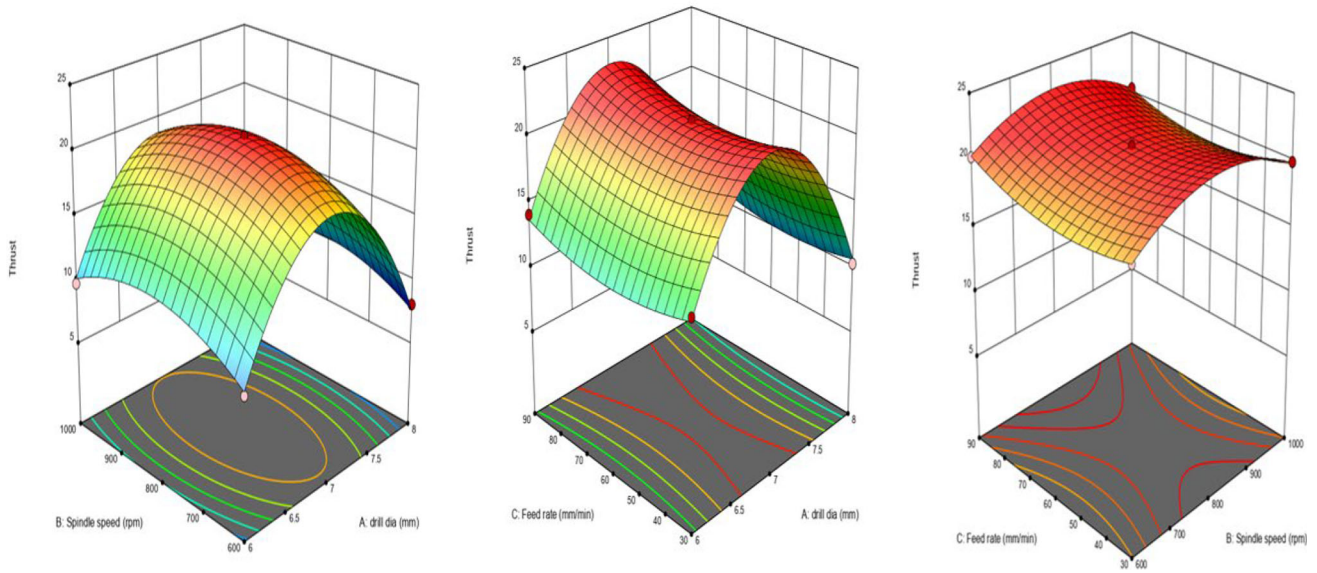


Fig. 4 3D surface plots for various parameters for thrust force

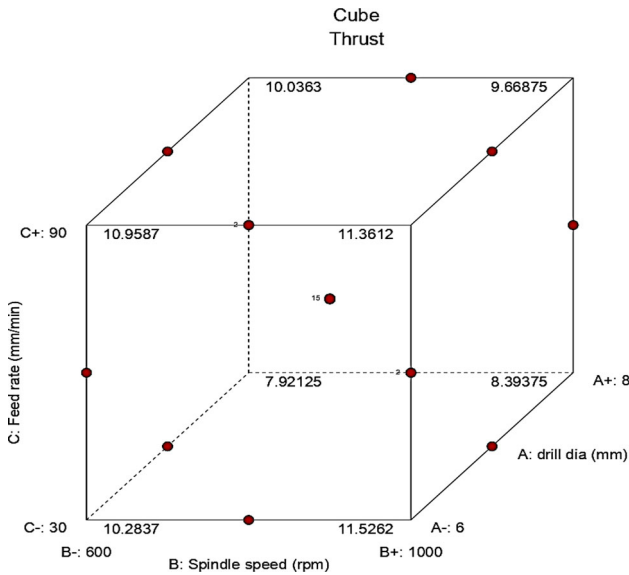


Fig. 5 Cube for identifying the various points

3.2 ANOVA analysis for thrust force

ANOVA was employed to identify primary factors and evaluate their statistically significant interaction at a confidence level of 95%. A p-value threshold of ≤ 0.05 indicates significant effects of the main parameters (drill diameter, spindle speed, feed rate, or their interactions) on both thrust force and surface roughness. The p-value for the interaction term is less than 0.0001, signifying a significant influence of the considered process factors on thrust force [23]. Here, the model F-value is obtained as 1204.56, which is larger and highly significant for thrust force, corresponding to a P-value less than

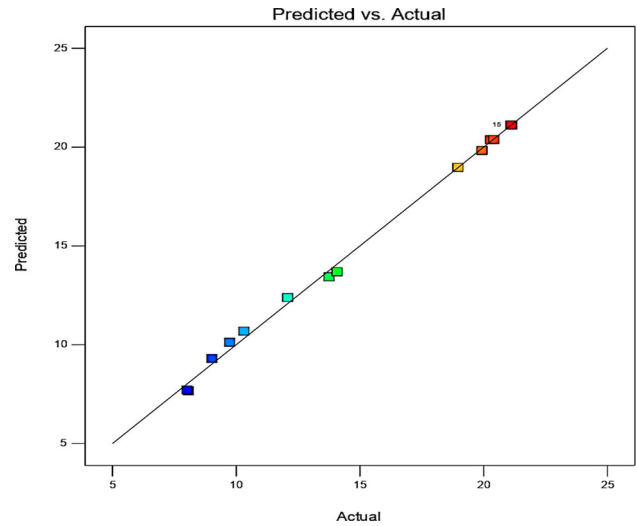


Fig. 6 Predicted vs actual values plot for thrust force

0.0001. Among other noise sources, the model shows values of 140.37 for drill diameter and 32.46 for feed rate, which are significant factors. Similarly, the nonlinear quadratic mathematical model of A^2 , B^2 , and C^2 leads to the most significant contributing factors, shown in the F-value, compared to the interactions AB, AC, and BC, which are non-significant. The overall p-value, alpha, is less than 0.005, indicating statistical significance. According to the ANOVA results, drill diameter emerged as the most significant parameter, suggesting that the proposed model holds substantial validity for predicting thrust force.

The model variables denoted as A^2 , B^2 , C^2 , AC, A, B, C, and D are noticed to have an evident effect on thrust force due to their p-values being less than 0.05; on the contrary,

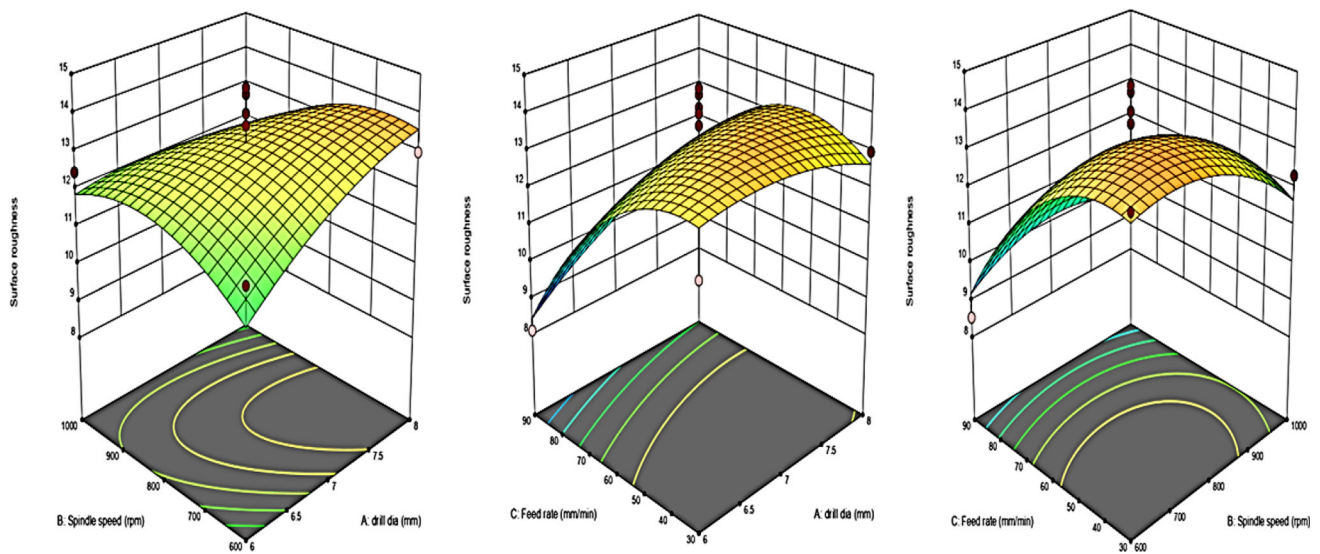


Fig. 7 3D surface plots for various parameters for Surface Roughness

p-values more prominent than 0.1 indicate that the factors in the portrait are not imperative, (it is also supported by Fedai et al. [8]). R^2 and adj. R^2 was determined to have values of 0.9984 and 0.9749, respectively, close to unity. The minimal deviation between R^2 and Adj R^2 indicates that the model is suited for the current data and may predict future observations (Antil et al., 2022).

3.3 Analysis of result for surface roughness

Figure 7 presents the synergy plot depicting the relationship between spindle speed and drill. Examination of Fig. 7a indicates that the amalgamation of spindle speed and drill correlates with reduced surface roughness values. Particularly, the lowest surface roughness, falling between 11 and 12 Kgf, was attained at elevated values of spindle speed (1000 rpm) and drill diameter (8 mm). This observation is corroborated by findings from Barailly et al. [4]. The possible reason may be attributed to the fact that the higher feed rate at the drill values of 6 mm and 8 mm has gradually enhanced, and hence, lower surface roughness has been attained. However, at the central point of the feed rate, a curve is shown due to rises in temperature at higher spindle speeds along with drill diameter, which cut polymer composites. In these situations, the surface removal chip of particles adheres to the drill diameter, which does not correctly evacuate the surface hole quality of the composite polymer material. Beyond this, in Fig. 7b and c, lower surface roughness has been produced at the gradual rises of feed rate and spindle speed, which depicted those lower losses of thermal energy at the interaction of drill diameter at a surface roughness value of 8 and 9. Figure 7a, b, and c illustrate a decreasing trend in average surface roughness with rising spindle speed and an increasing trend with higher

feed rate values. Thus, it is observed that increasing spindle speed up to a certain threshold positively impacts the surface quality of composite polymer holes [24].

In contour plots, Fig. 7, the interactions between spindle speed and drill diameter show that the combination of drill diameter and spindle speed can lead to the machined hole being the worst due to the evacuation of fiber sticks on the rake face. Thermal softening generates heat energy on this rake face and gradually widens the machined holes. Therefore, increasing the drill diameter while decreasing the spindle speed produces uniform machined holes on jute fiber. However, it can be argued that achieving minimal surface roughness entails using a larger drill diameter, a reduced feed rate, and a lower spindle speed, which facilitates the creation of uniform fiber holes. This, in turn, diminishes the normal pressure applied to the rake face of the drill diameter and enhances the surface finish of the holes in the jute fiber composite.

Figure 8 displays the plot comparing predicted and actual surface roughness (μm). The data exhibits a linear trend, suggesting the model's validity. Additionally, the normal probability plots of performance attributes, as depicted in Fig. 8, reveal that residuals conform to a linear pattern, indicating a normal distribution of errors [36]. Furthermore, Fig. 8 illustrates that most of the surface roughness predicted by the RSM aligns with the regression line, resulting in an overall R-value of 0.8111. Consequently, the RSM model effectively establishes the correlation between surface roughness and drill process parameters. Nonetheless, it demonstrates reduced predictive capability compared to GRA and optimization models, as evidenced by findings from Paturi et al. [30].

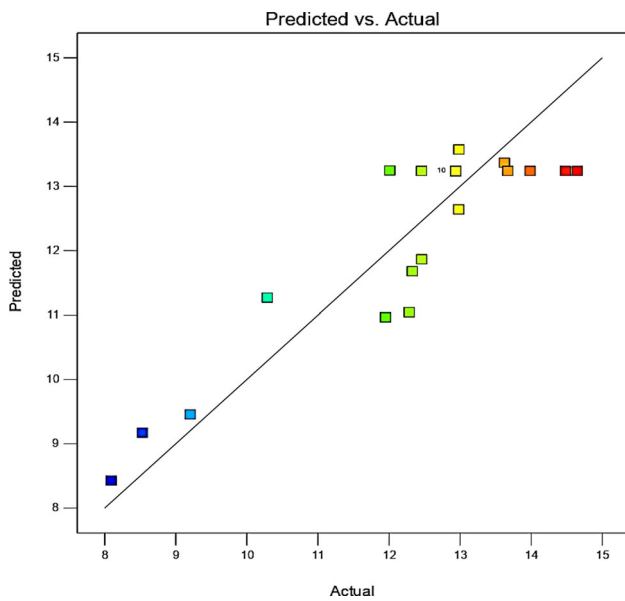


Fig. 8 Predicted vs actual values graph for surface roughness

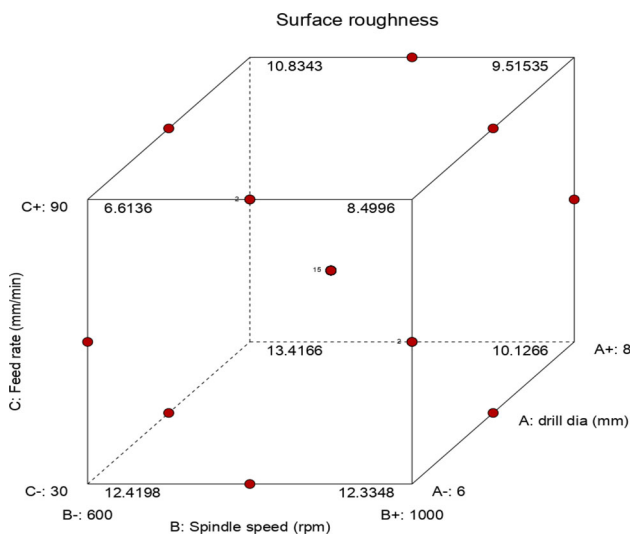


Fig. 9 Various points of Cube for surface roughness

In the recent investigation, drill experiments have been carried out on polymer composites using BBD. BBD is a response surface design broadly employed for managing non-linear models. A one-factor-at-a-time response approach is included to select the baseline levels for each aspect. The cube plot in Fig. 9 shows the variation in Ra with all dominant parameters. Examining the cube plot, it is observed that with a 6 mm drill diameter and a spindle speed of 600 rpm, increasing the feed rate from 30 to 90 mm/min results in the Ra values rising from 9.50 to 10.90 μm . Therefore, the cubic region indicates that all the tested points fall within predefined boundaries. In cases where out-of-bounds trials

are prevented by virtual boundaries, the BBD technique is suggested.

3.4 ANOVA analysis for surface roughness

Table 4 illustrates the statistical analysis using ANOVA for surface roughness (SR). The regression framework term and all other design factors significantly influenced the SR values [6]. In our study, the overall model for surface roughness yielded an F-value of 8.11, with a p-value < 0.001 , indicating statistical significance and the model's importance. This reaffirms the reasonable accuracy and overall effectiveness of the nonlinear polynomial model.

The feed rate exerted the most substantial influence (30.64%), followed by drill diameter (3.02%) and spindle speed (1.46%), with the highest F-value recorded at 27.58. The p-value of SR for LOF is 0.0101, affirming the model's adequacy, supported by findings from Kumar et al. [20]. Furthermore, examining R² values underscores the framework's suitability, with R² and adjusted R² for SR standing at 0.7111 and 0.8111, respectively. The noticeable deviation between R² and Adj. R² suggests the model accurately fits the current data and can reliably predict future observations. Additionally, the minor standard deviation of 0.864 confirms that SR's maximum variation is 0.864 μm . In light of these SR results, predicting response values within the selected range is feasible using the regression equation provided in Eq. (8).

Equations (7) and (8) display the derived regression equation model for thrust force and surface roughness. According to the ANOVA table, the suggested model is significant, with feed rate and drill diameter being determined as the most crucial parameters.

3.5 Thrust force and surface roughness—regression models

The experiments were assessed using the BBD design in conjunction with RSM, resulting in significant findings. A second-order polynomial equation, incorporating all three independent parameters and their interactions, was derived. The resulting RSM equations, presented in Eq. (7) for thrust force and Eq. (8) for surface roughness [30], depict precise mathematical relationships that enable the prediction of these parameters with known coefficients. Utilizing regression equations facilitates the optimization of adaptive evolutionary algorithms, namely GA and TLBO, providing high-quality and global solutions. While GA relies on a random search of historical data, TLBO operates iteratively to enhance computational efficiency and expert consistency. MATLAB Software version R2020b employs the problem-based solver optimization tool for accurate and precise computations, utilizing experimental variables, responses,

Table 4 Analysis of variance for surface roughness

| Source | Sum of squares | D.F | Mean square | F-value | P-value | |
|-----------------|----------------|--------------------------|-------------|---------|----------|-------------|
| Model | 54.5 | 9 | 6.06 | 8.11 | 0.0001 | Significant |
| A-Drill dia | 2.03 | 1 | 2.03 | 2.71 | 0.1179 | |
| B-Spindle speed | 0.9856 | 1 | 0.9856 | 1.32 | 0.2665 | |
| C-Feed rate | 20.59 | 1 | 20.59 | 27.58 | < 0.0001 | Significant |
| AB | 2.57 | 1 | 2.57 | 3.44 | 0.0811 | |
| AC | 2.6 | 1 | 2.6 | 3.48 | 0.0794 | |
| BC | 0.9712 | 1 | 0.9712 | 1.3 | 0.2698 | |
| A ² | 0.9925 | 1 | 0.9925 | 1.33 | 0.2648 | |
| B ² | 3.71 | 1 | 3.71 | 4.98 | 0.0395 | |
| C ² | 10.29 | 1 | 10.29 | 13.79 | 0.0017 | |
| Residual | 12.69 | 17 | 0.7465 | | | |
| Lack of Fit | 6.9 | 3 | 2.3 | 5.55 | 0.0101 | Significant |
| Pure error | 5.8 | 14 | 0.414 | | | |
| Cor total | | | | | | |
| Fit statistics | 67.19 | 26 | | | | |
| Std. dev | 0.864 | R ² | | | 0.8111 | |
| Mean | 12.42 | Adjusted R ² | | | 0.7111 | |
| C.V. % | 6.96 | Predicted R ² | | | -0.7409 | |
| | | Adeq Precision | | | 9.7897 | |

and regression equations to construct the fitness function.

$$\begin{aligned}
 Thrustforce = & 21.1199999999997442 + \\
 & -1.013749999999926015 * A \\
 & + 0.2187500000000155431 * B \\
 & + 0.4875000000000032196 * C + \\
 & -0.19250000000000699885 * AB \\
 & + 0.3600000000000131894 * AC \\
 & + -0.2100000000000051958 * BC \\
 & + -9.876250000000077449 * A^2 \\
 & + -2.536250000000007816 * B^2 \\
 & + 1.311249999999989164 * C^2
 \end{aligned} \quad (7)$$

$$\begin{aligned}
 SurfaceRoughness = & 13.2407999999999302 \\
 & + 0.5031250000000326406 * A + \\
 & -0.3509999999999687006 * B + \\
 & -1.60437500000001066 * C + \\
 & -0.8012500000000690115 * AB \\
 & + 0.805999999999949463 * AC \\
 & + 0.492749999999957723 * BC \\
 & + -0.4501500000000210401 * A^2
 \end{aligned}$$

$$\begin{aligned}
 & + -0.87090000000000256097 * B^2 \\
 & + -1.449649999999978847 * C^2
 \end{aligned} \quad (8)$$

3.6 Genetic algorithm optimization

The regression modeling equations generated by the nonlinear method for the reactions are refined using the MOGA process. The findings of Pareto analysis using the MOGA technique are shown in Fig. 10. The minimization equations for thrust and surface roughness responses are represented by functions 1 and 2. The data were entered into the GA's optimization toolbox, accessible through MATLAB, by creating fitness functions. According to the specifications, a problem-based solver was chosen, and MOGA was selected for this investigation. All required data were input into the Graphical User Interface (GUI) window for the present work. After choosing the population size in MATLAB, the Solver was run, results were plotted, and the data were exported into the Workbench window of the MATLAB.

Figure 10 displays the function values and decision variables acquired by the MOGA technique. The comparison of the outcomes using various strategies is shown in Table 5.

Fig. 10 Best fitness, Current best individual response plot in GA optimization for Thrust

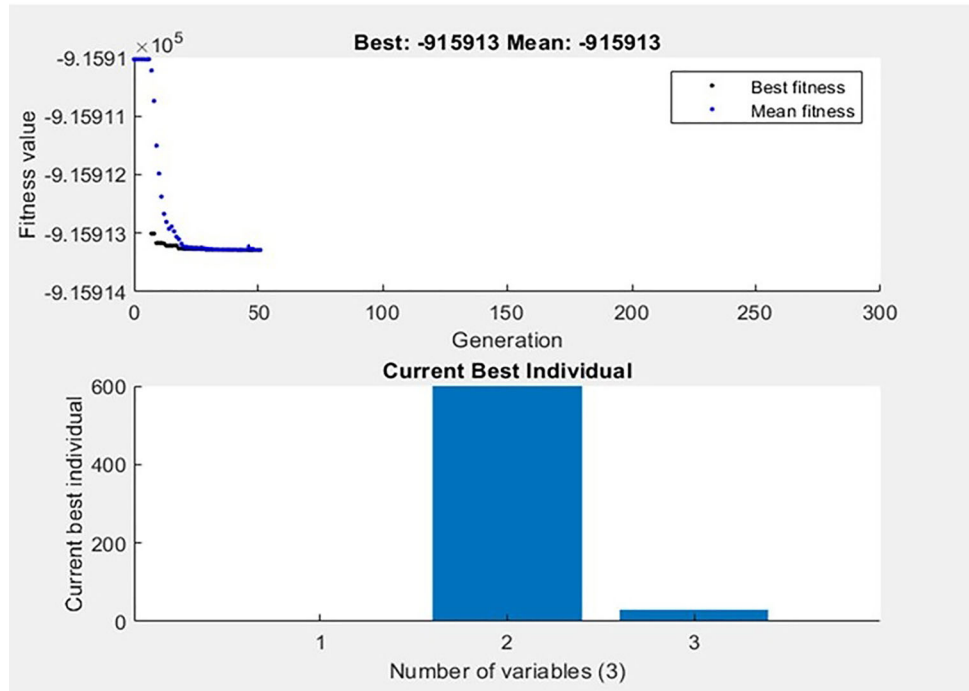


Table 5 Comparison sheet for process parameters at Min (Thrust and SR) Predicted by GRA, GA and TLBO

| Comparison sheet output | Composite polymer | | | | |
|-------------------------|-------------------|----------------------------|-------------------|---------------|-------------------------|
| | Algorithm | Optimal process parameters | | | |
| | | Drill μs | Spindle speed Rpm | Feed rate Amp | Fitness function (Min.) |
| Thrust (Kgf) | GRA | 8 | 1400 | 30 | 6.92 |
| | GA | 6 | 600 | 30 | $-9.1589e + 05$ |
| | TLBO | 8 | 1400 | 90 | -4.989×10^{-6} |
| SR (μm) | GRA | 7 | 1400 | 60 | 8.048 |
| | GA | 6 | 600 | 30 | $-3.0758e + 05$ |
| | TLBO | 8 | 1400 | 90 | -1.696×10^{-6} |

The default value and configuration are maintained for all GA parameters, including population type and size, creation, crossover, selection, and mutation. After 50 iterations, the fitness function’s lowest value was found; this number is indicated for ease of visualization because the fitness function’s value remains roughly constant after this point. After a thorough estimation, the ideal configuration for the drill step variables emerged, and the related outcome was recorded. The convergence plot of thrust and SR in GA is depicted in Fig. 11, where the best means for thrust are at -9.15912 , and the best means for SR are at -3.07592 .

Solve for:
A, B, C

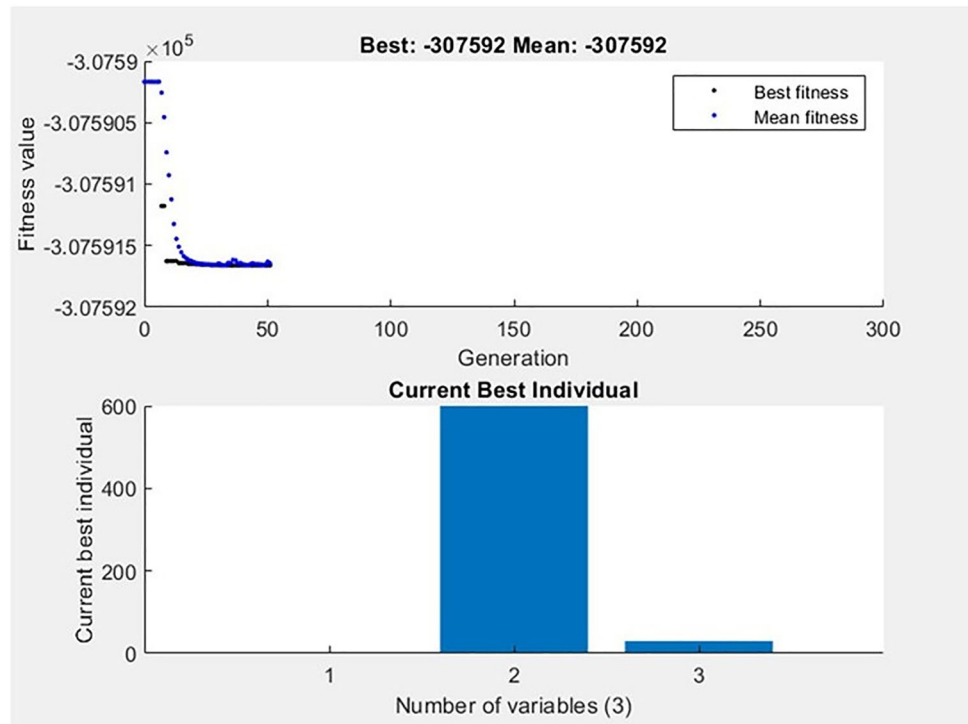
Where, A: Drill, B: Spindle, C: Feed rate

$$\begin{aligned}
 & \text{Fitnessfunction}(\text{minimizeThrust}) \\
 & = -9.8763 * A^2 - 2.5363 * B^2 + 1.3112 * C^2 \\
 & \quad - 0.1925 * A * B - 0.21 * B * C + 0.36 * A * C \\
 & \quad - 1.0137 * A + 0.21875 * B + 0.4875 * C + 21.12 \quad (9)
 \end{aligned}$$

$$\begin{aligned}
 & \text{Fitnessfunction}(\text{minimizeSR}) \\
 & = -0.45015 * A^2 - 0.8709 * B^2 - 1.4496 * C^2 \\
 & \quad - 0.80125 * A * B + 0.49275 * B * C + 0.806 * A * C \\
 & \quad + 0.50313 * A - 0.351 * B - 1.6044 * C + 13.2408 \quad (10)
 \end{aligned}$$

The chosen GA setting that is subject to limitations is:

Fig. 11 Best fitness, Current best individual response plot in GA optimization for Surface roughness



constraint1: $A \leq 3$; constraint2: $B \leq 600$ constraint3: $C \leq 30$

variable bounds : $3 \leq A \leq 9$ (11)

$600 \leq B \leq 1400$ (12)

$30 \leq C \leq 90$ (13)

3.7 Single objective optimization using TLBO algorithm

The TLBO algorithm is executed by treating each response as a positive integer. Limits were applied to the parameters of the drill process after machining, and then the algorithms were executed.

(Drill): $6 \text{ mm} \leq \text{Drill} \leq 8 \text{ mm}$

(Spindle Speed): $600 \text{ rpm} \leq \text{Spindle} \leq 1400 \text{ rpm}$

(Feed Rate): $30 \text{ mm/min} \leq \text{Feed rate} \leq 90 \text{ mm/min}$

Single-objective optimization of response characteristics occurred with a TLBO approach to minimize thrust and SR. It was investigated whether three machining variables—feed rate, spindle rate, and drill rate—affect the expected response parameters. Table 5 provides the effects of optimization. Single-objective optimization findings indicate that a minimum thrust of -4.99×10^{-6} Kgf and a minimum SR of -1.695×10^{-6} μm were generated within the preferred range

of machining characteristics. The results clearly show that as the thickness and surface roughness increase, the thrust and surface roughness also attain minimum values, which is desirable. However, the minimum viable values for drill, spindle, and feed rates have been set at 8 and 90, respectively. However, this compromises both thrust and SR, as the lowest possible values achieved are -4.99×10^{-6} Kgf and -1.695×10^{-6} μm . Therefore, it can be seen that there is a conflict between the response parameters, and the single-objective optimization result enables the user to choose the machining variables to minimize one of the response parameters. Trade-offs between these aspects must be resolved to arrive at an advantageous set of parametric parameters that can be employed for drill technology. A multi-objective optimization strategy can tackle the problem and eliminate such complexity. The MOTLBO strategy has been used to conduct simultaneous optimization by assigning equal weights of 0.50 to the finalized responses. A population size of 27 and several iterations of 50 are specified, and these are accomplished after executing a few trials to attempt to achieve the ideal setting for individual responses utilizing the TLBO algorithm. Table 5 illustrates the optimum scores for thrust and SR. As seen in Figs. 12 and 13, a convergence graph is drawn amid the response variables (thrust and SR) and the number of iterations. The algorithm has been accomplished 50 times to assess the stability of the TLBO anticipated results. Next, the standard deviation and average findings are documented. For thrust, the average result after 50 trials is -4.989×10^{-6} Kgf; for surface roughness, it is -1.696

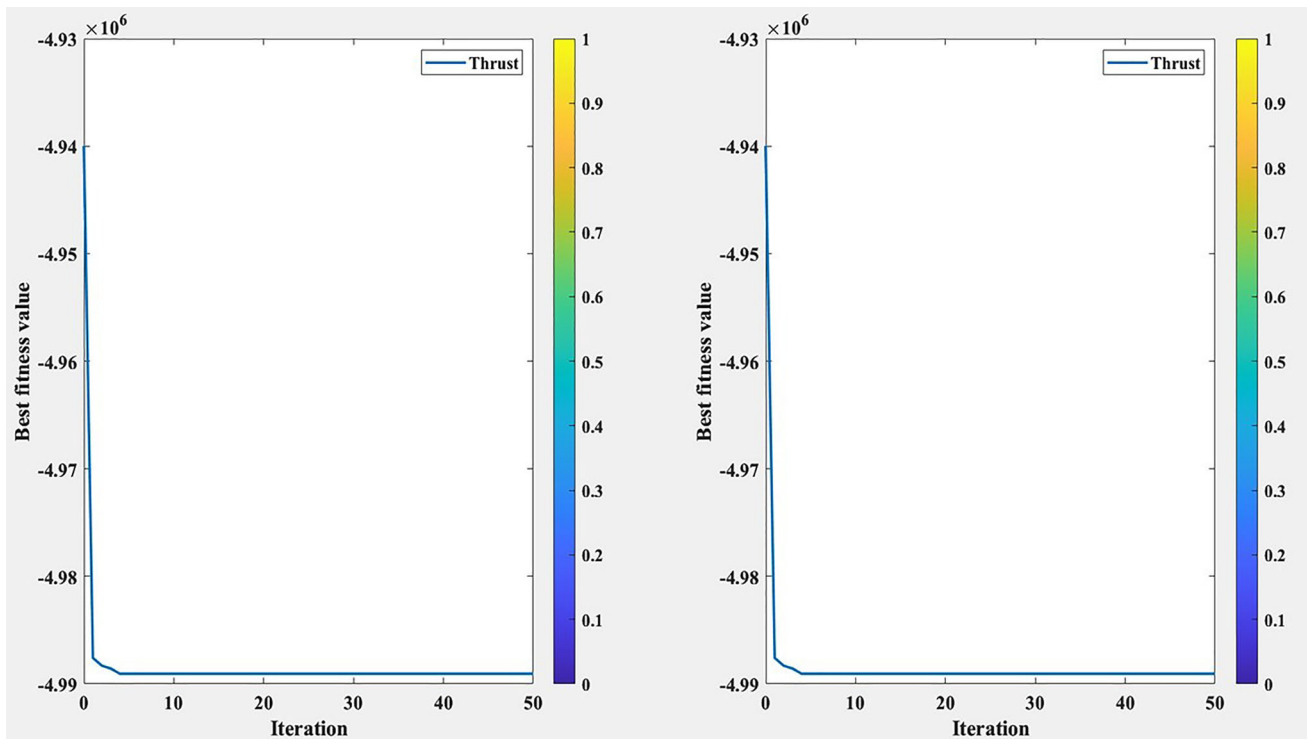


Fig. 12 TLBO Convergence curve for composite polymer a Thrust

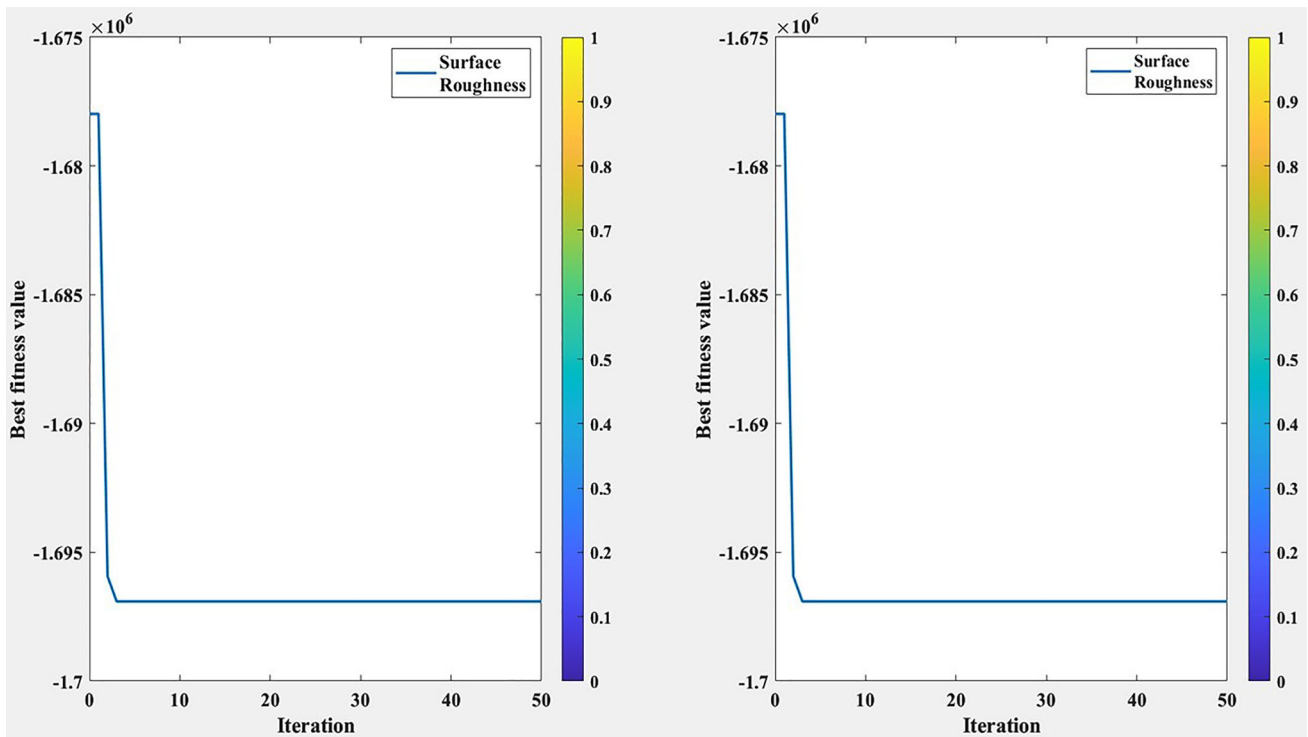


Fig. 13 TLBO Convergence curve for composite polymer a Surface Roughness

× 10–6 μm. The average of 50 runs is closer to the optimal consequence for both scenarios.

3.8 A comparative investigation of the projected outcomes of GRA with GA and TLBO predicted outcomes

The effectiveness of the TLBO algorithm is validated through five repetitions, matching the experimental configurations outlined in Table 5. Minimal disparities between the experimental and TLBO-predicted outcomes are noted, with experimental discrepancies of 4.63% for thrust and 3.45% for surface roughness (SR). These discrepancies, falling below 5%, are considered noteworthy [36]. Comparative evaluation of output responses, as illustrated in Table 5, indicates a close correspondence between the TLBO-predicted results and experimental observations.

In comparison, the fitness function sheet responds to the availability and functionality relationship between parameters and features by employing MCDM of GRA and global optimization of GA and TLBO. Here, the GRA technique is mainly used to make decisions involving multiple criteria rather than directly optimizing complex objective functions. It can deal with high-dimensional and nonlinear optimization problems. Furthermore, GA and TLBO are suitable for complex optimization problems involving ample search space and non-linear relationships [5]. They employ population-based strategies and stochastic operators to explore the solution space effectively.

4 Conclusion and recommendations

The study performed on the polymeric composite showed that using drilling operations on different diameters significantly plays a significant role in machinability and tool wear. It further emerged that the thrust force value may be decreased even more by employing the proper settings. The integrated technique is relatively broad with numerous machining characteristics applied to GA and TLBO optimization. It may be utilized as a potent prototype for the modelling and optimization of any drilling and machining operation. The optimal GA and TLBO results produce the best fitness statistic, and its validation reveals the closer outcome. The following determination has been reached:

1. The study investigated the impact of process parameters (drill diameter, spindle speed, and feed rate) on response characteristics (thrust force and surface roughness). ANOVA regression analysis highlighted the significance of these factors, with p-values < 0.05 for both thrust force and surface roughness (SR). Notably, drill diameter and feed rate demonstrated significant f-values (37

and 32.36, respectively) for thrust force, while feed rate (27.39) was influential for surface roughness. Residual plots confirmed the robustness of multivariable relationships and the reliability of ANOVA statistics, enhancing future result prediction.

2. Optimization studies aim to collectively enhance economic, environmental, and social considerations to define the optimal process parameters for sustainable component manufacturing. In this context, in the scenarios involving a 6 mm drill diameter, a spindle speed of 600 mm/rev, and a feed rate of 30 amp, the GRA outcomes yield superior results compared to GA. The optimal response parameters are thrust force -9.1589×10^5 Kgf and $R_a = -3.0758 \times 10^5$ μm. A 4% discrepancy in the confirmed GA results validates the algorithm's effectiveness and enhances its convergence capabilities.
3. The single-objective optimization results from TLBO show a minimum SR of 1.696 μm (responses with a drill diameter of 8 μs, spindle speed of 1400 rpm, and feed rate of 90 amp). Similarly, single-objective optimization successes from TLBO predict a minimum thrust of 4.989 Kgf at the same input responses.
4. It was identified that the measured responses were well within a 5% fluctuation, and the experimental results agreed well with the optimization results. The statistical regression model and the TLBO strategy are effective when there is the slightest error between anticipated and accurate data.
5. Based on the DoE strategy, the current effort is concentrated. Additional methods for advanced hybrid optimization can be employed for future research projects, including manufacturing advanced composite polymers.
6. A parallel approach can explore the impact of drill machining parameters like tool geometry and feed rate. Future investigations could delve into statistical variables and additional responses, such as delamination at entry and exit, as well as temperature and pressure exerted on the drill tool, across advanced reinforced jute and glass fiber composites. Moreover, comprehensive experimental studies are necessary to assess the applicability and effectiveness of various multi-optimization techniques.

Funding No funding is received for this research work and publication.

Data availability The data used to support the findings of this study are included in the article.

Declarations

Conflicts of interest The authors declare that there are no conflicts of interest regarding the publication of this paper.

References

1. Antil, P., Singh, S., Manna, A.: Electrochemical discharge drilling of SiC reinforced polymer matrix composite using Taguchi's grey relational analysis. *Arab. J. Sci. Eng.* **43**(3), 1257–1266 (2018)
2. Antil, P., Singh, S., Manna, A., Katal, N., Pruncu, C.: An improvement in drilling of SiCp/glass fiber-reinforced polymer matrix composites using response surface methodology and multi-objective particle swarm optimization. *Polym. Compos.* **42**(10), 5051–5064 (2021)
3. Babu, U.H., Sai, N.V., Sahu, R.K.: Artificial intelligence system approach for optimization of drilling parameters of glass-carbon fiber/polymer composites. *SILICON* **13**(9), 2943–2957 (2021)
4. Baraily, A., Chatterjee, S., Ghadai, R. K., Das, P. P., & Chakraborty, S.: Optimization of hybrid Al-MMC drilling using a new RAMS-RATMI-based approach. *Int. J. Interact. Des. Manuf. (IJIDeM)*, pp. 1–17, (2023)
5. Belaadi, A., Boumaaza, M., Alshahrani, H., Bourchak, M.: Effect of jute fiber length on drilling performance of biocomposites: optimization comparison between RSM, ANN, and genetic algorithm. *Int. J. Adv. Manuf. Technol.* **124**(10), 3579–3599 (2023)
6. Chaudhari, R., Ayesta, I., Doshi, M., Khanna, S., Patel, V.K., Vora, J., De Lacalle, L.N.L.: Effect of Multi-walled carbon nanotubes on the performance evaluation of Nickel-based super-alloy–Udimet 720 machined using WEDM process. *Int. J. Adv. Manuf. Technol.* **123**(5), 2087–2105 (2022)
7. Erturk, A.T., Vatanserver, F., Yazar, E., Guven, E.A., Sinmazcelik, T.: Effects of cutting temperature and process optimization in drilling of GFRP composites. *J. Compos. Mater.* **55**(2), 235–249 (2021)
8. Fedai, Y.: Optimization of drilling parameters in drilling of MWCNT-reinforced GFRP nanocomposites using Fuzzy AHP-weighted taguchi-based MCDM methods. *Processes* **11**(10), 2872 (2023)
9. Fedai, Y., Basar, G., Kirli Akin, H.: Multi-response optimization in drilling of MWCNTs reinforced GFRP using grey relational Analysis. *Tehnički vjesnik* **29**(3), 742–751 (2022)
10. Feito, N., Muñoz-Sánchez, A., Díaz-Álvarez, A., Miguelez, M.H.: Multi-objective optimization analysis of cutting parameters when drilling composite materials with special geometry drills. *Compos. Struct.* **225**, 111187 (2019)
11. Geier, N., Szalay, T.: Optimisation of process parameters for the orbital and conventional drilling of uni-directional carbon fibre-reinforced polymers (UD-CFRP). *Measurement* **110**, 319–334 (2017)
12. Gupta, A., Vaishya, R., Kumar, R., Khan, K. L. A., Chhabra, S., Verma, A. S., & Bharadwaj, A.: Effect of drilling process parameters on delamination factor in drilling of pultruded glass fiber reinforced polymer composite. *Mater. Today Proc.* (2022)
13. Heidary, H., Karimi, N.Z., Minak, G.: Investigation on delamination and flexural properties in drilling of carbon nanotube/polymer composites. *Compos. Struct.* **201**, 112–120 (2018)
14. Ismail, S.O., Sarfraz, S., Niamat, M., Mia, M., Gupta, M.K., Pimenov, D.Y., Shehab, E.: Comprehensive study on tool wear during machining of fiber-reinforced polymeric composites. In: Sultan, M.T.H. (ed.) *Machining and Machinability of Fiber Reinforced Polymer Composites*, pp. 129–147. Springer, Singapore (2021)
15. Jayabal, S., Natarajan, U.: Optimization of thrust force, torque, and tool wear in drilling of coir fiber-reinforced composites using Nelder-Mead and genetic algorithm methods. *Int. J. Adv. Manuf. Technol.* **51**(1), 371–381 (2010)
16. Jayaprakash, V., Sivasaravanan, S., Raja, V.B., Anish, M., Raman, N., Laxman, N.: Optimization of drilling parameters of epoxy/rice husk composite material. *Mater. Today Proc.* **21**, 104–107 (2020)
17. Kaviarasan, V., Venkatesan, R., Natarajan, E.: Prediction of surface quality and optimization of process parameters in drilling of Delrin using neural network. *Progr. Rubber Plast. Recycl. Technol.* **35**(3), 149–169 (2019)
18. Kharwar, P.K., Verma, R.K.: Machining performance optimization in drilling of multiwall carbon nano tube/epoxy nanocomposites using GRA-PCA hybrid approach. *Measurement* **158**, 107701 (2020)
19. Krishnaraj, V., Prabukarhi, A., Ramanathan, A., Elanghovan, N., Kumar, M.S., Zitoun, R., Davim, J.P.: Optimization of machining parameters at high speed drilling of carbon fiber reinforced plastic (CFRP) laminates. *Compos. B Eng.* **43**(4), 1791–1799 (2012)
20. Kumar, A., Sharma, R., Gujral, R.: Investigation of crack density, white layer thickness, and material characterization of biocompatible material commercially pure titanium (grade-2) through a wire electric discharge machining process using a response surface methodology. *Proc. Instit. Mech. Eng. Part E J. Process Mech. Eng.* **235**(6), 2073–2097 (2021)
21. Kumar, J., Kesarwani, S., Kharwar, P.K., Jackson, M.J., Verma, R.K.: Mechanical performance and drilling machinability evaluation of carbon nano onions (CNOs) reinforced polymer nanocomposites. *Int. J. Interact. Des. Manuf. (IJIDeM)* **17**(1), 169–186 (2023)
22. Makhesana, M. A., Bagga, P. J., Agrawal, M. K., Mangukiya, J., Patel, R., Patel, K. M., & Dwivedi, Y. D.: Investigation on the effect of process parameters and optimization using GRA under biodegradable oil based MQL in machining. *Int. J. Interact. Des. Manuf. (IJIDeM)*, pp. 1–12, (2023)
23. Malik, K., Ahmad, F., Keong, W.T., Gunister, E.: The effects of drilling parameters on thrust force, temperature and hole quality of glass fiber reinforced polymer composites. *Polym. Polym. Compos.* **30**, 09673911221131113 (2022)
24. Meral, G., Sankaya, M., Mia, M., Dilipak, H., Şeker, U., Gupta, M.K.: Multi-objective optimization of surface roughness, thrust force, and torque produced by novel drill geometries using Taguchi-based GRA. *Int. J. Adv. Manuf. Technol.* **101**, 1595–1610 (2019)
25. Mercy, J.L., Prakash, S., Krishnamoorthy, A., Ramesh, S., Anand, D.A.: Experimental investigation and multiresponse genetic optimization of drilling parameters for self-healing GFRP. *J. Mech. Sci. Technol.* **31**(8), 3777–3785 (2017)
26. Niranjana, T., Singaravel, B., & Raju, S. S.: Optimization of hole quality parameters using TOPSIS method in drilling of GFRP composite. *Materials Today: Proc.* (2022)
27. Palanikumar, K.: Experimental investigation and optimisation in drilling of GFRP composites. *Measurement* **44**(10), 2138–2148 (2011)
28. Palanikumar, K., Latha, B., Senthilkumar, V.S., Davim, J.P.: Analysis on drilling of glass fiber–reinforced polymer (GFRP) composites using grey relational analysis. *Mater. Manuf. Processes* **27**(3), 297–305 (2012)
29. Panneerselvam, T., Raghuraman, S., Kandavel, T.K., Mahalingam, K.: Evaluation and analysis of delamination during drilling on sisal-glass fibres reinforced polymer. *Measurement* **154**, 107462 (2020)
30. Paturi, U.M.R., Cheruku, S., Pasunuri, V.P.K., Salike, S., Reddy, N.S., Cheruku, S.: Machine learning and statistical approach in modeling and optimization of surface roughness in wire electrical discharge machining. *Mach. Learn. Appl.* **6**, 100099 (2021)
31. Rababah, M.M., AL-Oqla, F.M., Wasif, M.: Application of analytical hierarchy process for the determination of green polymeric-based composite manufacturing process. *Int. J. Interact. Des. Manuf. (IJIDeM)* **16**(3), 943–954 (2022)
32. Ramesh, B., Elayaperumal, A., Satishkumar, S., Kumar, A., Jayakumar, T.: Effect of drill point geometry on quality characteristics and multiple performance optimization in drilling of nonlaminated composites. *Proc. Inst. Mech. Eng. Part L J. Mater. Des. Appl.* **230**(2), 558–568 (2016)

33. Ramesh, B., Kumar, S. S., Elsheikh, A. H., Mayakannan, S., Sivakumar, K., & Duraitilagar, S.: Optimization and experimental analysis of drilling process parameters in radial drilling machine for glass fiber/nano granite particle reinforced epoxy composites. In: *Materials Today: Proceedings* (2022)
34. Rezghi Maleki, H., Hamed, M., Kubouchi, M., Arao, Y.: Experimental study on drilling of jute fiber reinforced polymer composites. *J. Compos. Mater.* **53**(3), 283–295 (2019)
35. Saravanakumar, A., & Reddy, S. A.: Optimization of process parameter in drilling of snake grass fiber reinforced composites. *Mater. Today Proc.* **62**(8), 5460–5466 (2022)
36. Sharma, P., Chakradhar, D., Narendranath, S.: Measurement of WEDM performance characteristics of aero-engine alloy using RSM-based TLBO algorithm. *Measurement* **179**, 109483 (2021)
37. Shunmugesh, K., Pratheesh, A.: Taguchi grey relational analysis based optimization of micro-drilling parameters on carbon fiber reinforced plastics. *Mater. Today Proc.* **24**, 1994–2003 (2020)
38. Soepangkat, B.O., Pramujati, B., Effendi, M.K., Norcahyo, R., Mufarrih, A.M.: Multi-objective optimization in drilling kevlar fiber reinforced polymer using grey fuzzy analysis and Back-propagation Neural Network-Genetic Algorithm (BPNN-GA) Approaches. *Int. J. Precis. Eng. Manuf.* **20**(4), 593–607 (2019)
39. Soleymani Yazdi, M.R., Razfar, M.R., Asadnia, M.: Modelling of the thrust force of the drilling operation on PA6–nanoclay nanocomposites using particle swarm optimization. *Proc. Inst. Mech. Eng. Part B J. Eng. Manuf.* **225**(10), 1757–1771 (2011)
40. Uysal, A., Altan, M., Altan, E.: Effects of cutting parameters on tool wear in drilling of polymer composite by Taguchi method. *Int. J. Adv. Manufact. Technol.* **58**(9), 915–921 (2012)
41. Vinayagamoorthy, R., Manoj, I.V., Narendra Kumar, G., Sai Chand, I., Kumar, S.C., et al.: A central composite design based fuzzy logic for optimization of drilling parameters on natural fiber reinforced composite. *J. Mech. Sci. Technol.* **32**(5), 2011–2020 (2018)

Publisher's Note Springer Nature remains neutral with regard to jurisdictional claims in published maps and institutional affiliations.

Springer Nature or its licensor (e.g. a society or other partner) holds exclusive rights to this article under a publishing agreement with the author(s) or other rightsholder(s); author self-archiving of the accepted manuscript version of this article is solely governed by the terms of such publishing agreement and applicable law.